

# The Contribution of Multiparametric Pelvic and Whole-Body MRI to Interpretation of <sup>18</sup>F-Fluoromethylcholine or <sup>68</sup>Ga-HBED-CC PSMA-11 PET/CT in Patients with Biochemical Failure After Radical Prostatectomy

Ur Metser<sup>1</sup>, Sue Chua<sup>2</sup>, Bao Ho<sup>3</sup>, Shonit Punwani<sup>4</sup>, Edward Johnston<sup>4</sup>, Frederic Pouliot<sup>5</sup>, Noam Tau<sup>1</sup>, Asmaa Hawsawy<sup>1</sup>, Reut Anconina<sup>1</sup>, Glenn Bauman<sup>6</sup>, Rodney J. Hicks<sup>7</sup>, Andrew Weickhardt<sup>8</sup>, Ian D. Davis<sup>9</sup>, Greg Pond<sup>10</sup>, Andrew M. Scott<sup>8</sup>, Nina Tunariu<sup>2</sup>, Harbir Sidhu<sup>4</sup>, and Louise Emmett<sup>3</sup>

<sup>1</sup>University of Toronto, Toronto, Canada; <sup>2</sup>Royal Marsden Hospital, London, United Kingdom; <sup>3</sup>St. Vincent's Hospital, Sydney, Australia; <sup>4</sup>University College London, London, United Kingdom; <sup>5</sup>Université Laval, Quebec, Canada; <sup>6</sup>London Health Sciences Centre, Ontario, Canada; <sup>7</sup>Peter MacCallum Cancer Centre, Melbourne, Australia; <sup>8</sup>Austin Health, Melbourne, Australia; <sup>9</sup>Eastern Health Clinical School, Monash University, Box Hill, Victoria, Australia; and <sup>10</sup>McMaster University, Hamilton, Ontario Canada;

Our purpose was to assess whether the addition of data from multiparametric pelvic MRI (mpMR) and whole-body MRI (wbMR) to the interpretation of <sup>18</sup>F-fluoromethylcholine (<sup>18</sup>F-FCH) or <sup>68</sup>Ga-HBED-CC PSMA-11 (<sup>68</sup>Ga-PSMA) PET/CT (=PET) improves the detection of local tumor recurrence or of nodal and distant metastases in patients after radical prostatectomy with biochemical failure. **Methods:** The current analysis was performed as part of a prospective, multicenter trial on <sup>18</sup>F-FCH or <sup>68</sup>Ga-PSMA PET, mpMR, and wbMR. Eligible men had an elevated level of prostate-specific antigen (PSA) (>0.2 ng/mL) and high-risk features (Gleason score > 7, PSA doubling time < 10 mo, or PSA > 1.0 ng/mL) with negative or equivocal conventional imaging results. PET was interpreted with mpMR and wbMR in consensus by 2 radiologists and compared with prospective interpretation of PET or MRI alone. Performance measures of each modality (PET, MRI, and PET/mpMR–wbMR) were compared for each radiotracer and each individual patient (for <sup>18</sup>F-FCH, or <sup>68</sup>Ga-PSMA for patients who had <sup>68</sup>Ga-PSMA PET) and to a composite reference standard. **Results:** There were 86 patients with PET (<sup>18</sup>F-FCH [*n* = 76] and/or <sup>68</sup>Ga-PSMA [*n* = 26]) who had mpMR and wbMR. Local tumor recurrence was detected in 20 of 76 (26.3%) on <sup>18</sup>F-FCH PET/mpMR, versus 11 of 76 (14.5%) on <sup>18</sup>F-FCH PET (*P* = 0.039), and in 11 of 26 (42.3%) on <sup>68</sup>Ga-PSMA PET/mpMR, versus 6 of 26 (23.1%) on <sup>68</sup>Ga-PSMA PET (*P* = 0.074). Per patient, PET/mpMR was more often positive for local tumor recurrence than PET (*P* = 0.039) or mpMR (*P* = 0.019). There were 20 of 86 patients (23.3%) with regional nodal metastases on both PET/wbMR and PET (*P* = 1.0) but only 12 of 86 (14%) on wbMR (*P* = 0.061). Similarly, there were more nonregional metastases detected on PET/wbMR than on PET (*P* = 0.683) or wbMR (*P* = 0.074), but these differences did not reach significance. Compared with the composite reference standard for the detection of disease beyond the prostatic fossa, PET/wbMR, PET, and wbMR had sensitivity of 50%, 50%, and 8.3%, respectively, and specificity of 97.1%, 97.1%, and 94.1%, respectively. **Conclusion:** Interpretation of

PET/mpMR resulted in a higher detection rate for local tumor recurrence in the prostatic bed in men with biochemical failure after radical prostatectomy. However, the addition of wbMR to <sup>18</sup>F-FCH or <sup>68</sup>Ga-PSMA PET did not improve detection of regional or distant metastases.

**Key Words:** prostate cancer; biochemical recurrence; MR; PSMA; fluoromethylcholine; PET

**J Nucl Med 2019; 60:1253–1258**

DOI: 10.2967/jnumed.118.225185

**W**e recently published the results of an international, multicenter trial on <sup>18</sup>F-fluoromethylcholine (<sup>18</sup>F-FCH) or <sup>68</sup>Ga-HBED-CC PSMA-11 (<sup>68</sup>Ga-PSMA) PET/CT (=PET) and multiparametric pelvic MRI (mpMR) in men with high-risk features and biochemical failure after radical prostatectomy. The study showed that both <sup>18</sup>F-FCH and <sup>68</sup>Ga-PSMA PET had a high detection rate for extraprostatic fossa disease in men with negative or equivocal conventional imaging results and biochemical recurrence after radical prostatectomy. This affected management and treatment responses to salvage fossa radiotherapy, suggesting an important role for PET in triaging men being considered for curative radiotherapy (1). Study patients underwent mpMR to assess for local tumor recurrence and whole-body MRI (wbMR) to assess for nodal and distant metastases. mpMR has been previously validated as a robust imaging modality for detection of local recurrence in the prostatic bed in men after radical prostatectomy for prostate cancer with biochemical failure, even at low serum levels of prostate-specific antigen (PSA), and may help predict response to salvage radiotherapy (2). Comparison of mpMR to <sup>18</sup>F-FCH PET has shown comparable results (3,4). Some authors have suggested that combining PET and MRI would yield better results (3). The purpose of the current analysis was to determine whether the addition of data from mpMR and wbMR to the interpretation of <sup>18</sup>F-FCH or <sup>68</sup>Ga-PSMA PET would improve the detection of local tumor recurrence or of nodal and distant metastases in this patient population.

Received Dec. 20, 2018; revision accepted Jan. 30, 2019.  
For correspondence or reprints contact: Ur Metser, University of Toronto, 610 University Ave., Suite 3-960, Toronto, ON, M5G 2M9, Canada.  
E-mail: ur.metser@uhn.ca  
Published online Mar. 22, 2019.  
COPYRIGHT © 2019 by the Society of Nuclear Medicine and Molecular Imaging.

## MATERIALS AND METHODS

This prospective, international multicenter trial was approved by all institutional ethics boards (clinicaltrials.gov identifier NCT02131649). Ninety-one eligible, consenting men with biochemical failure after radical prostatectomy and high-risk features being considered for curative-intent salvage fossa radiotherapy were prospectively recruited across the 8 participating sites in Australia, Canada, and the United Kingdom between July 2014 and January 2017. All patients had biopsy-confirmed prostate cancer, prior radical prostatectomy for pT1–T3, N0/Nx disease, a rising serum PSA level of at least 0.2 ng/mL (3 consecutive rises documented a minimum of 2 wk apart), and at least one high-risk feature (PSA > 1.0 ng/mL, stage  $\geq$  pT3b, Gleason score > 7, or PSA doubling time  $\leq$  10 mo). Negative or equivocal CT and bone scan results within 12 wk of enrollment were required. Exclusion criteria included significant sarcomatoid or spindle cell or neuroendocrine small cell components, proven metastatic disease, evidence of unequivocal disease outside the prostatic bed on conventional imaging, and refusal of salvage prostatic bed radiotherapy or androgen deprivation therapy within 6 mo before enrollment. Study interventions comprised  $^{18}\text{F}$ -FCH PET, mpMR, and wbMR within a 2-wk period, with men in Australia undergoing an additional  $^{68}\text{Ga}$ -PSMA PET scan within the same time frame.

### Image Interpretation

PET was prospectively interpreted in consensus by experienced readers locally and at a central site (Peter MacCallum Cancer Centre). mpMR was read in consensus by 2 local radiologists with expertise in interpretation of prostate MRI, and the wbMR was interpreted centrally (University College London and Royal Marsden). The interpretation criteria, using a 4-point certainty scale, were previously described (*1*). In brief, focal radiotracer uptake in the prostatic bed or a nodule with intermediate–high T2 signal abnormality, and early arterial-phase enhancement on dynamic contrast-enhanced MRI, were considered positive for local tumor recurrence. Lymph nodes were considered positive if distinct radiotracer uptake was identified, excluding nodes at sites where reactive lymphadenopathy is common, such as the groin. Focal skeletal uptake above background marrow activity and or a focus of signal abnormality on MRI, especially if associated with restricted diffusion, were considered positive for bone metastasis unless explained by a benign abnormality such as fracture or degenerative change.

All imaging results were uploaded to a central database. For the current analysis, a combined interpretation of PET/mpMR–wbMR was performed independently by 2 of 3 board-certified readers experienced in interpreting PET and MRI. The readers were able to review all datasets (PET, mpMR, and wbMR) on dedicated workstations. Results were tabulated by a further radiologist, who identified discordance between the readers in the detection of local tumor recurrence or of nodal or distant metastatic disease. Discordant cases were re-reviewed by the original readers. If a consensus could not be reached, a third, tie-breaker, independent read was obtained. The combined PET/mpMR–wbMR read was compared with prospective PET and mpMR and wbMR interpretation.

### Imaging Acquisition Protocols

**PET.** All men underwent immediate dynamic pelvic (10 min) and then delayed whole-body PET with coverage from skull base to proximal thighs at 60 min after intravenous administration of  $^{18}\text{F}$ -FCH (3.6 MBq/kg to a maximum of 400 MBq at the time of injection). A low-dose, unenhanced CT scan was initially performed for attenuation correction and localization. The initial dynamic acquisition was acquired over the pelvis at  $4 \times 30$  s,  $4 \times 1$  min, and  $2 \times 2$  min. Subsequently, the whole-body PET acquisition was obtained. In those undergoing  $^{68}\text{Ga}$ -PSMA PET, imaging from vertex to mid thighs was undertaken at least

60 min after the intravenous administration of  $^{68}\text{Ga}$ -PSMA HBEDD-11 (2.0 MBq/kg, to a maximum 200 MBq at the time of injection). The images were stored on a centralized secure server for central review.

**mpMR.** mpMR was performed per local institutional protocols but was harmonized to include small-field-of-view, T2-weighted axial and coronal sequences, axial dynamic contrast-enhanced sequences after administration of gadolinium-based contrast, and optional axial sequences with b50 and b1,000 s/mm<sup>2</sup> diffusion weighting. After acquisition, the images were uploaded to a centralized online secure server and centrally reviewed for quality.

**wbMR.** The wbMR acquisition included Dixon or T1-weighted imaging and axial diffusion-weighted imaging at 1.5 or 3 T using gradients of b50 and b1,000 s/mm<sup>2</sup> with coverage from skull base to mid thighs. For T1-weighted imaging, precontrast fat-saturated volume-interpolated gradient-echo imaging (3-dimensional) was performed, and a Dixon-based technique was preferred. Imaging was performed either in the coronal plane using an isotropic image resolution of 2 or 3 mm adjusted to allow a maximum breath-hold time for acquisitions of 20 s per station, or in the axial plane with a 5-mm slice thickness. For diffusion-weighted imaging, any fat saturation technique could be used with a slice thickness of 5–7 mm.

### Composite Reference Standard

In accord with the study protocol, biopsy of imaging-positive lesions was encouraged but not mandated. Overall, 12% of men (11/91) underwent biopsy of scan-positive sites of disease. The composite standard reference incorporating biopsy and targeted treatment response was presented in detail in our prior publication (*1*). In brief, patients with positive imaging for disease beyond the prostatic fossa were considered true-positive for metastatic disease if biopsy confirmed the findings or if an insufficient therapeutic response to pelvic radiotherapy only was observed. Patients with imaging negative for disease beyond the prostatic fossa were considered true-negative if a therapeutic response was observed. Patients who received androgen deprivation therapy without a biopsy outside the prostatic bed and patients who underwent surveillance without having a biopsy performed outside the prostatic bed were excluded. Treatment response was defined as a drop in PSA level of more than 50% from pretreatment levels in the absence of androgen deprivation therapy at the time of PSA assessment at least 6 mo after treatment. Men who were placed

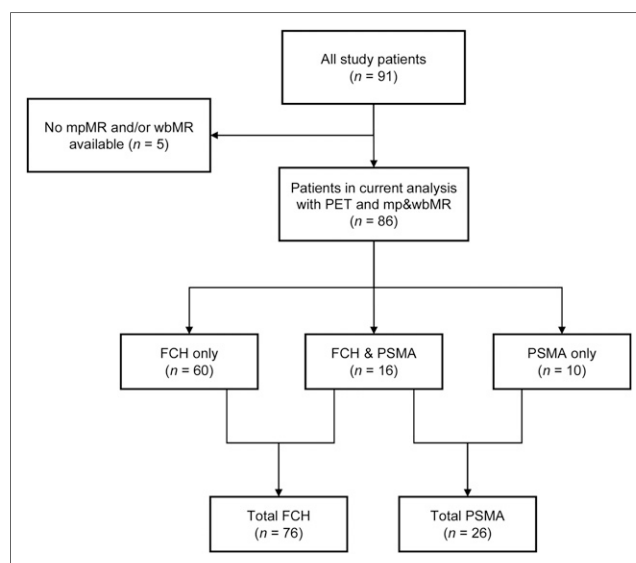


**FIGURE 1.** Flowchart depicting study patients included and radiopharmaceuticals used.

**TABLE 1**

Detection of Local Tumor Recurrence in Prostate Bed for <sup>18</sup>F-FCH or <sup>68</sup>Ga-PSMA PET/mpMR Versus PET or mpMR Alone

Parameter	PET/mpMR (+)	PET/mpMR (-)	Total
<b><sup>18</sup>F-FCH or <sup>68</sup>Ga-PSMA PET/mpMR vs. PET*</b>			
PET (+)	13 (15.1%)	3 (3.5%)	16 (18.6%)
PET (-)	12 (14%)	58 (67.4%)	70 (81.4%)
Total	25 (29.1%)	61 (70.9%)	86 (100%)
<b><sup>18</sup>F-FCH or <sup>68</sup>Ga-PSMA PET/mpMR vs. mpMR†</b>			
mpMR (+)	8 (9.3%)	5 (5.8%)	13 (15.1%)
mpMR(-)	17 (19.8%)	56 (65.1%)	73 (84.9%)
Total	25 (29.1%)	61 (70.9%)	86 (100%)

\**P* = 0.039.  
†*P* = 0.019.

on androgen deprivation therapy as part of treatment were not included in the assessment of initial treatment response.

**Data Comparisons and Statistical Analysis**

The detection of local tumor recurrence in the prostatic bed was compared for each modality (PET, mpMR, and PET/mpMR) and for each radiopharmaceutical separately. Furthermore, detection of local tumor recurrence for each modality was compared for individual patients. In the latter comparison, for patients who had both <sup>18</sup>F-FCH and <sup>68</sup>Ga-PSMA PET, only <sup>68</sup>Ga-PSMA PET data were used. Similarly, the detection of disease beyond the prostatic fossa was compared on PET, wbMR, and PET/wbMR for each radiopharmaceutical and for individual patients. Finally, for the detection of disease beyond the prostatic fossa, the diagnostic accuracy of each modality (sensitivity, specificity, positive predictive value, negative predictive value, and accuracy) was determined using the composite reference standard described above. The detection rates of the different imaging modalities were compared using a 2-sided McNemar  $\chi^2$  test. A *P* value of 0.05 or less was deemed statistically significant.

**RESULTS**

The study included 91 patients with a median age of 64 y (interquartile range, 59–69 y) and a median of 23 mo (interquartile range, 9–46.5 mo) from radical prostatectomy. These patients had

stage T2 (34/91, 37.5%), T3a (35/91, 39.5%), or T3b (21/91, 23%) tumors and a Gleason score of 6–7 in 60 of the 91 patients (67%) or 8–10 in 29 of the 91 (32%). The median PSA level at the time of imaging was 0.42 ng/mL (interquartile range, 0.29–0.93 ng/mL), and the median PSA doubling time was 5 mo (interquartile range, 3.3–7.6 mo). Further details on patient demographics, including therapy received after PET, were previously published (1). Complete imaging datasets (PET, mpMR, and wbMR) were available for 86 of the 91 patients (94.5%). There were 102 PET scans for these patients, including 76 of 86 <sup>18</sup>F-FCH PET (88.4%) and 26 of 86 <sup>68</sup>Ga-PSMA PET (30.2%) (Fig. 1).

**Combined PET/mpMR–wbMR Interpretation**

Initial interpretation by 2 of 3 independent reviewers was concordant in 64 of 102 datasets (62.8%). Most discordant lesions were in the prostatic bed (25/38; 65.8%). Consensus was reached in a second review of imaging by the same 2 reviewers in 33 of 38 discordant PET/mpMR–wbMR datasets (86.8%). A third independent interpretation was used to adjudicate the remaining discordant cases.

**Local Recurrence in Prostatic Bed**

*For Each Modality and Radiopharmaceutical.* <sup>18</sup>F-FCH PET/mpMR was more frequently positive for local tumor recurrence in the prostatic bed than <sup>18</sup>F-FCH PET (20/76 [26.3%] vs. 11/76

**TABLE 2**

Detection of Regional Nodal Metastases for <sup>18</sup>F-FCH or <sup>68</sup>Ga-PSMA PET/wbMR Versus PET or wbMR Alone

Parameter	PET/wbMR (+)	PET/wbMR (-)	Total
<b><sup>18</sup>F-FCH or <sup>68</sup>Ga-PSMA PET/wbMR vs. PET*</b>			
PET (+)	18 (21%)	2 (2.3%)	20 (23.3%)
PET (-)	2 (2.3%)	64 (74.4%)	66 (76.7%)
Total	20 (23.3%)	66 (76.7%)	86 (100%)
<b><sup>18</sup>F-FCH or <sup>68</sup>Ga-PSMA PET/wbMR vs. wbMR†</b>			
wbMR (+)	9 (10.5%)	3 (3.5%)	12 (14%)
wbMR (-)	11 (12.8%)	63 (73.3%)	74 (86.1%)
Total	20 (23.3%)	66 (76.7%)	86 (100%)

\**P* = 1.0.  
†*P* = 0.061.

TABLE 3

Detection of Nonregional Nodal and Distant Metastases for <sup>18</sup>F-FCH or <sup>68</sup>Ga-PSMA PET/wbMR Versus PET or wbMR Alone

Parameter	PET/wbMR (+)	PET/wbMR (-)	Total
<b><sup>18</sup>F-FCH or <sup>68</sup>Ga-PSMA PET/wbMR vs. PET*</b>			
PET (+)	2 (2.3%)	2 (2.3%)	4 (4.7%)
PET (-)	4 (4.7%)	78 (90.7%)	82 (95.3%)
Total	6 (7%)	80 (93%)	86 (100%)
<b><sup>18</sup>F-FCH or <sup>68</sup>Ga-PSMA PET/wbMR vs. wbMR†</b>			
wbMR (+)	1 (1.2%)	0 (0%)	1 (1.2%)
wbMR (-)	5 (5.8%)	80 (93%)	85 (98.8%)
Total	6 (7%)	80 (93%)	86 (100%)

\**P* = 0.683.  
†*P* = 0.074.

[14.5%], respectively); only 8 were concordant (*P* = 0.039; odds ratio [OR], 0.25; 95% confidence interval [CI], 0.045–0.926). Similarly, <sup>68</sup>Ga-PSMA PET/mpMR was more often positive for local tumor recurrence in the prostatic bed than <sup>68</sup>Ga-PSMA PET (11/26 [42.3%] vs. 6/26 [23.1%], respectively); however, this difference did not reach significance for the current cohort (*P* = 0.074; OR, 0; 95% CI, 0–1.091).

**For Individual Patients.** The detection of local tumor recurrence on PET/mpMR and PET or mpMR interpreted separately was performed for 86 unique patients. For patients who had both <sup>68</sup>Ga-PSMA and <sup>18</sup>F-FCH PET, only data from <sup>68</sup>Ga-PSMA PET were used for this analysis. Overall, there were 26 of 86 patients (30.2%) with <sup>68</sup>Ga-PSMA PET/mpMR and 60 of 86 patients (69.8%) with <sup>18</sup>F-FCH PET/mpMR (Table 1). PET/mpMR was more often positive for local tumor recurrence than PET alone (*P* = 0.039; OR, 4; 95% CI, 1.079–22.088) or mpMR (*P* = 0.019; OR, 0.294; 95% CI, 0.085–0.831).

#### Presence of Nodal or Distant Metastases

The detection of nodal metastases for each modality (PET/wbMR, PET, and wbMR) is presented in Table 2. There were 20 patients with regional nodal metastases on both PET and PET/wbMR, and 18 of these were concordant (*P* = 1.0; OR, 1; 95% CI, 0.072–13.796). PET/wbMR suggested more regional nodal metastases than wbMR (20/86 [23.3%] vs. 12/86 [14%], respectively); however, this difference did not reach significance (*P* = 0.061; OR, 0.273; 95% CI, 0.049–1.032). Only 9 of 32 patients (28.1%) suggested as having nodal metastases with either modality were positive on both.

The detection of nonregional nodal (M1a category) and distant (M1b, M1c) metastases is presented in Table 3. There were more M1a–M1c metastases detected on PET/wbMR than on PET

(*P* = 0.683; OR, 0.5; 95% CI, 0.045–3.489) or wbMR (*P* = 0.074; OR, 0; 95% CI, 0–1.091), but this difference was not significant.

#### Nodal or Distant Metastases Compared with Composite Reference Standard

Of the 86 study patients, 58 had a composite standard of reference available for the presence of disease beyond the prostatic fossa (Table 4). The performance measures of <sup>18</sup>F-FCH or <sup>68</sup>Ga-PSMA PET/wbMR were similar to those of <sup>18</sup>F-FCH or <sup>68</sup>Ga-PSMA PET, with discordance in 3 cases only. The sensitivity, specificity, positive predictive value, negative predictive value, and overall accuracy for both modalities (PET and PET/wbMR) were 50%, 97.1%, 92.3%, 73.3%, and 77.6%, respectively. The performance measures for wbMR for detection of disease beyond the prostatic fossa were generally inferior to PET and PET/wbMR, with a sensitivity, specificity, positive predictive value, negative predictive value, and overall accuracy of 8.3%, 94.1%, 50%, 59.3%, and 58.6%, respectively.

#### DISCUSSION

The role of PET/MRI in oncology is evolving. A recent review of initial PET/MRI studies in over 2,300 patients has suggested that PET/MRI has similar diagnostic performance to PET/CT (5). In patients with prostate cancer, MRI may have an advantage over CT in detecting tumor in the prostate or prostatic fossa and in detecting bone metastases; however, the incremental value of MRI to information provided from PET remains uncertain and likely varies according to the specific clinical scenario. The current study assessed the contribution of data obtained from mpMR and wbMR to <sup>18</sup>F-FCH or <sup>68</sup>Ga-PSMA PET in assessing local tumor recurrence and metastases in men with biochemical failure

TABLE 4

Metastatic Disease: Comparison of <sup>18</sup>F-FCH or <sup>68</sup>Ga-PSMA PET, PET/wbMR, or wbMR to Composite Reference Standard

Parameter	True-positive	True-negative	False-negative	False-positive
<sup>18</sup> F-FCH or <sup>68</sup> Ga-PSMA PET	12 (20.7%)	33 (56.9%)	12 (20.7%)	1 (1.7%)
wbMR	2 (3.5%)	32 (55.2%)	22 (37.9%)	2 (3.5%)
<sup>18</sup> F-FCH or <sup>68</sup> Ga-PSMA PET/wbMR	12 (20.7%)	33 (56.9%)	12 (20.7%)	1 (1.7%)

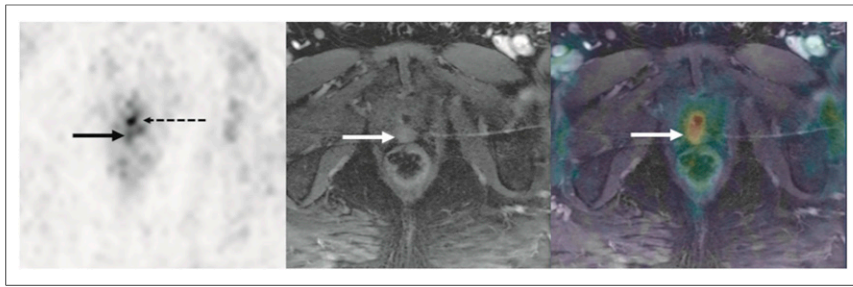


**FIGURE 2.** Axial  $^{68}\text{Ga}$ -PSMA PET (left), mpMR (middle), and fused (right) images of 65-y-old man after radical prostatectomy with biochemical recurrence (PSA, 1.1 ng/mL). PET shows intense radiotracer activity (dashed arrow) in urethra at level of surgical anastomosis and ill-defined moderate uptake (solid black arrow) posterior to urethra, not interpreted prospectively as tumor on PET. Fused image shows that radiotracer uptake corresponds to focus of abnormal enhancement on mpMR image (white arrows), suggestive of local tumor recurrence.

after radical prostatectomy. Of note, in our study, mpMR and wbMR were acquired separately from PET rather than with a hybrid PET/MRI scanner. Dedicated fusion software enabled multimodality image fusion when needed.

Previous studies have shown that when the serum PSA level is 1 ng/mL or less, mpMR detects local recurrence in the prostatic bed in 11%–21% of patients (6,7). Our results were similar, with a detection rate of 15.1% for the entire cohort. The addition of mpMR data to PET nearly doubled tumor detection for both  $^{18}\text{F}$ -FCH and  $^{68}\text{Ga}$ -PSMA PET, with PET/mpMR outperforming PET alone or mpMR alone. Interpretation of local tumor recurrence in the prostatic fossa may be challenging, and this represented the most common site for discordance between readers at PET/mpMR. These findings are in line with a previously published study in which a head-to-head comparison of  $^{11}\text{C}$ -choline PET/MRI and  $^{11}\text{C}$ -choline PET/CT in 75 patients with biochemical failure showed that local tumor recurrence was identified more often on PET/MRI than on PET/CT (8). The improved lesion detection with PET/mpMR over PET and mpMR alone may be explained by the moderately high sensitivity of both modalities in identifying local tumor recurrence while exploiting different tumor characteristics (Fig. 2). For example, mpMR could demonstrate tumor nodules that are masked by urine activity in the urethra on PET. In other instances, the presence of an abnormality on both imaging modalities, albeit subtle in some cases, may enable a more confident diagnosis of local tumor recurrence (Fig. 3).

Overall, wbMR identified nodal or distant metastases in 13 of 86 patients (15.1%) in our study, similar to results in a previous trial, in which metastases were identified in 13.2% of patients (7). When PET findings were interpreted in conjunction with wbMR findings, wbMR did not significantly contribute to the overall performance of PET in detecting lymph nodal or distant metastases. There are a few potential explanations for the limited contribution of wbMR data in this study. First,  $^{18}\text{F}$ -FCH and  $^{68}\text{Ga}$ -PSMA PET are more sensitive than wbMR in identifying nodal metastases, the most common metastatic site in this patient population (9,10). Second, the extended field of view of wbMR, typically from top of skull to upper thighs, limits the spatial resolution of wbMR. In our protocol, multiparametric, high-resolution, small-field-of-view imaging (mpMR) was obtained for the prostatic bed, but the wbMR was performed with a broader field of view and a slice thickness of up to 5–7 mm for diffusion-weighted imaging. The metastatic deposits beyond the prostatic fossa in this

patient population, who had negative or equivocal CT and bone scintigraphy findings, tend to be relatively small and prone to partial-volume effects with the wbMR parameters used, limiting lesion detectability. Furthermore, many wbMR protocols, including the one used in this trial, are lengthy, with an acquisition time of approximately 1 h or longer, depending on the number of sequences included. This may result in more frequent motion artifacts, which may further degrade image quality, especially for sequences with low signal-to-noise ratios, such as diffusion-weighted imaging (one of the imaging staples of the current wbMR protocol), or for small lesions (11,12). Our results suggest

that the sensitivity of hybrid imaging is likely driven by the more sensitive imaging modality, with a significant contribution from both modalities when detection is moderate or high with incomplete overlap in lesion detection, as was the case for detection of local tumor recurrence by PET/mpMR in our study. We were unable to demonstrate a benefit for the addition of wbMR to  $^{18}\text{F}$ -FCH or  $^{68}\text{Ga}$ -PSMA PET to guide therapy planning in men with biochemical failure after radical prostatectomy.

The main strengths of the current study include the collection of data from harmonized PET and MRI protocols across multiple centers across the world and the combination of local and central data analysis. However, the study does have several limitations. First, because of inclusion of multiple institutions with variable available imaging platforms, the PET and MRI data were obtained separately and not on integrated PET/MRI scanners. However, the

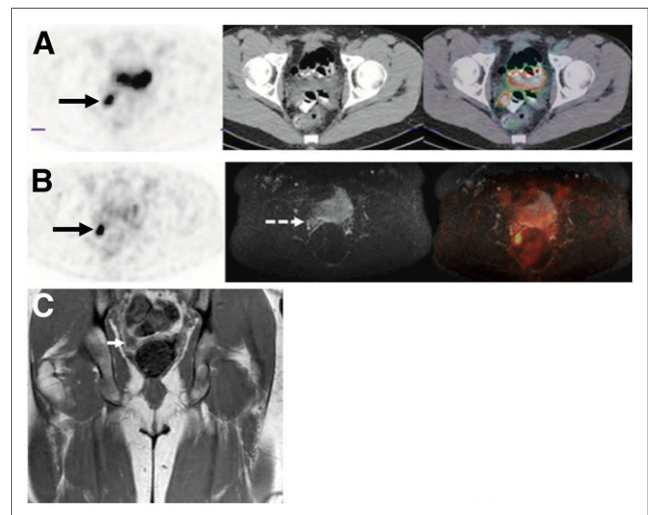


**FIGURE 3.** Images of 48-y-old man after radical prostatectomy with biochemical recurrence (serum PSA, 0.4 ng/mL). (A) On axial  $^{68}\text{Ga}$ -PSMA PET/CT (PET, left; CT, middle; fused, right), PET shows focal intense  $^{68}\text{Ga}$ -PSMA uptake in bed of right seminal vesicle (arrow), along cranial aspect of surgical clips (not shown). No definitive CT correlate could be identified. (B) On axial PET/MRI (PET, left; diffusion-weighted MRI [b1,000 s/mm<sup>2</sup>], middle; fused, right), focal intense PSMA uptake is seen in bed of right seminal vesicle (solid arrow) corresponding to focus of restricted diffusion on diffusion-weighted MRI. (C) This corresponds to a small soft-tissue nodule on coronal Dixon T1-weighted MR, not appreciated prospectively.

MRI protocol for the current study was developed to evaluate the prostatic fossa and remainder of body for recurrent or metastatic tumor, with similar coverage to that of  $^{18}\text{F}$ -FCH or  $^{68}\text{Ga}$ -PSMA PET, much akin to MRI obtained with integrated PET/MRI. Second, 2 different PET tracers were used in this study, with overlap in some patients. To overcome this limitation, we analyzed the performance measures of each tracer separately and assessed the performance measures for unique patients independently. These steps still may have resulted in limited statistical power, especially for  $^{68}\text{Ga}$ -PSMA, given its small number of patients in that cohort. Third, most lesions detected by each modality were not confirmed histologically. We did, however, use a composite reference standard, albeit imperfect, to compare the performance measures of PET, MRI, and PET/MRI for metastatic disease. This reference standard could not be used to determine whether PET or mpMR was correct in its characterization of the prostatic bed. Although PET/mpMR could improve detection of local recurrence in the prostatic bed, this improvement is unlikely to affect patient management because, in the absence of disease outside the prostatic fossa, patients would likely receive salvage pelvic radiotherapy.

## CONCLUSION

Interpretation of PET/mpMR resulted in a higher detection rate for local tumor recurrence in the prostatic bed in men with biochemical failure after radical prostatectomy. However, the addition of wbMR to  $^{18}\text{F}$ -FCH or  $^{68}\text{Ga}$ -PSMA PET did not improve detection of regional or distant metastases. These results may aid in refining PET/MRI protocols for this patient population.

## DISCLOSURE

Ian Davis is supported by an Australian National Health and Medical Research Council Practitioner Fellowship (APP1102604), as is Rodney Hicks (APP1108050). The work of Edward Johnston and Shonit Punwani is supported by the UCL/UCLH Biomedical Research Centre. Funding was provided by a GAP2 Collaborative Project Funding Award from the Movember Foundation. No other potential conflict of interest relevant to this article was reported.

## ACKNOWLEDGMENTS

We acknowledge the invaluable guidance and tireless support of Sam Gledhill of the Movember Foundation. Further thanks are given to the Society of Nuclear Medicine and Molecular Imaging team headed by Bonnie Clark for their role in the management of the imaging and data collection. We also acknowledge the support of local clinical trials teams in bringing together this project.

## KEY POINTS

**QUESTION:** Do data from mpMR or wbMR improve detection of tumor recurrence or metastases with  $^{18}\text{F}$ -FCH or  $^{68}\text{Ga}$ -PSMA PET in men with biochemical recurrence after radical prostatectomy?

**PERTINENT FINDINGS:** In this prospective multicenter trial, interpretation of PET with mpMR resulted in a higher detection rate for local tumor recurrence in the prostatic bed; however, the addition of wbMR to PET did not improve detection of regional or distant metastases.

**IMPLICATIONS FOR PATIENT CARE:** These results may aid in refining PET/MRI protocols for this patient population.

## REFERENCES

1. Emmett L, Metser U, Bauman G, et al. A prospective, multi-site, international comparison of F-18 fluoro-methyl-choline, multi-parametric magnetic resonance and Ga-68 HBED-CC (PSMA-11) in men with high-risk features and biochemical failure after radical prostatectomy: clinical performance and patient outcomes. *J Nucl Med*. November 15, 2018 [Epub ahead of print].
2. Sharma V, Nehra A, Colicchia M, et al. Multiparametric magnetic resonance imaging is an independent predictor of salvage radiotherapy outcomes after radical prostatectomy. *Eur Urol*. 2018;73:879–887.
3. Couñago F, Recio M, Maldonado A, et al. Evaluation of tumor recurrences after radical prostatectomy using  $^{18}\text{F}$ -choline PET/CT and 3T multiparametric MRI without endorectal coil: a single center experience. *Cancer Imaging*. 2016;16:42.
4. Sandgren K, Westerlinck P, Johsson JH, et al. Imaging for the detection of locoregional recurrences in biochemical progression after radical prostatectomy: a systematic review. *Eur Urol Focus*. November 11, 2017 [Epub ahead of print].
5. Spick C, Herrmann K, Czernin J.  $^{18}\text{F}$ -FDG PET/CT and PET/MRI perform equally well in cancer: evidence from studies on more than 2,300 patients. *J Nucl Med*. 2016;57:420–430.
6. Robertson NL, Sala E, Benz M, et al. Combined whole body and multiparametric prostate magnetic resonance imaging as a 1-step approach to the simultaneous assessment of local recurrence and metastatic disease after radical prostatectomy. *J Urol*. 2017;198:65–70.
7. Vargas HA, Martin-Malburet AG, Takeda T, et al. Localizing sites of disease in patients with rising serum prostate-specific antigen up to 1ng/ml following prostatectomy: how much information can conventional imaging provide? *Urol Oncol*. 2016;34:482.e5–482.e10.
8. Eiber M, Rauscher I, Souvatzoglou M, et al. Prospective head-to-head comparison of  $^{11}\text{C}$ -choline-PET/MR and  $^{11}\text{C}$ -choline-PET/CT for restaging of biochemical recurrent prostate cancer. *Eur J Nucl Med Mol Imaging*. 2017;44:2179–2188.
9. Metser U, Berlin A, Halankar J, et al.  $^{18}\text{F}$ -fluorocholine PET whole-body MRI in the staging of high-risk prostate cancer. *AJR*. 2018;210:635–640.
10. Gupta M, Choudhury PS, Hazarika D, Rawal S. A comparative study of  $^{68}\text{Ga}$ -gallium-prostate specific membrane antigen positron emission tomography-computed tomography and magnetic resonance imaging for lymph node staging in high risk prostate cancer patients: an initial experience. *World J Nucl Med*. 2017; 16:186–191.
11. Le Bihan D, Poupon C, Amadon A, Lethimonnier F. Artifacts and pitfalls in diffusion MRI. *J Magn Reson Imaging*. 2006;24:478–488.
12. Havsteen I, Ohlhues A, Madsen KH, Nybing JD, Christensen H, Christensen A. Are movement artifacts in magnetic resonance imaging a real problem?—A narrative review. *Front Neurol*. 2017;8:232.